USING DYNAMIC LIGHT SCATTERING PARTICLE SIZING AS A FAST SCREENING PROCEDURE FOR URINE SAMPLE ANALYSIS[#]

D. CHICEA, R. CHICEA**, LIANA MARIA CHICEA***

*Physics Department, "Lucian Blaga" University of Sibiu, 7–9, Dr. Ion Rațiu St., Sibiu, 550012, Romania, dan.chicea@ulbsibiu.ro
**"Victor Papilian" Faculty of Medicine, "Lucian Blaga" University of Sibiu

Abstract. A dynamic light scattering experiment was conducted on human urine. Results of particle size measurements are discussed in connection with the standard laboratory urine analysis output. A simple but very fast screening procedure is suggested.

Key words: dynamic light scattering, urine analysis.

INTRODUCTION

When a coherent light beam has a suspension as target, each particle in suspension scatters light. The coherent wavelets scattered by each scattering center (SC) interfere and the result is a speckled far field. References [5] and [10] describe the phenomenon. References [12, 13, 18, 19 20, 21] describe several procedures currently used for analyzing the speckle fluctuations and [8] presents in the introductory section a brief overview of the speckle analyses techniques. The most investigated biological particle in suspension is the red blood cell (RBC).

In this work a different biological fluid was used as target for the laser beam, namely human urine, both from healthy and unhealthy human subjects. Different particles and cells can be suspended in urine and act as SC. The experimental setup and a brief description of the Dynamic Light Scattering technique (DLS), the data processing procedure and the results are presented in the next sections.

[#]This study was presented as a poster in the *National Conference of Biophysics*, Cluj-Napoca, October, 2009.

Received October 2009;
in final form January 2010.

ROMANIAN J. BIOPHYS., Vol. 20, No. 3, P. 257–267, BUCHAREST, 2010

THE DYNAMIC LIGHT SCATTERING TECHNIQUE (DLS)

DLS is a well established technique for measuring particle size over a size range from nanometers to micrometers. As previously stated the light scattered by a suspension presents fluctuations [5, 10]. By placing a detector at a certain angle and recording the scattered light intensity a time series is recorded. As proved in [10, 22] the width of the autocorrelation function of the time series is proportional to the diffusion coefficient, which, in turn, depends on the hydrodynamic particle diameter. An improved version is described further on in this section.

Moving to details, the nanoparticles in aqueous solution undergo a three dimensional Brownian motion which is the cause of the nanoparticle diffusion. The early experimental works [9, 15] and the further theoretical treatises [4, 11, 12], proved the assumption that the power spectrum of the intensity of the light scattered by particles in suspension can be linked to the probability density function (PDF). This link between the PDF and the power spectrum is a consequence of the translation of the relative motion of the scattering particles into phase differences of the scattered light. Thus, spatial correlations are translated into phase correlations which are manifested in the usage of the Wiener-Khintchine-Theorem, relating the power spectrum to the autocorrelation of a process. The phase correlations lead to fluctuations in the intensity of the scattered light recorded using a detector and a data acquisition system, in a typical experimental setup as presented in Fig. 1.

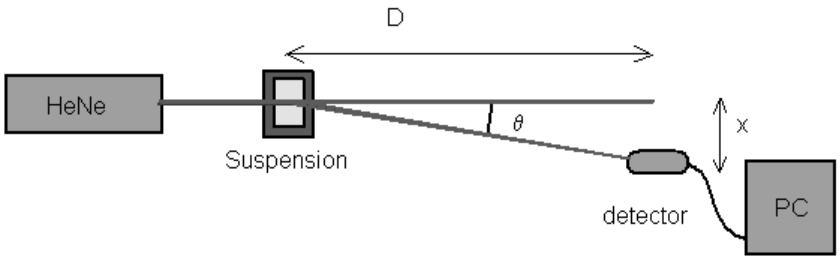

Fig. 1. A typical DLS experimental setup.

A sequence of a time series recorded for sample u6-2 is presented in Fig. 2. By subtracting the average intensity from the recorded time series and calculating the square of the intensity we obtain the power time series. The Fourier transform of the power time series is the power spectrum. We can compare the spectrum calculated from the experimental data with the theoretically expected spectrum, namely the functional form of the Lorentzian line $S(f)$ (Eq. 1).

$$S(f) = a_0 \frac{a_1}{(2\pi f) + a_1^2} \tag{1}$$

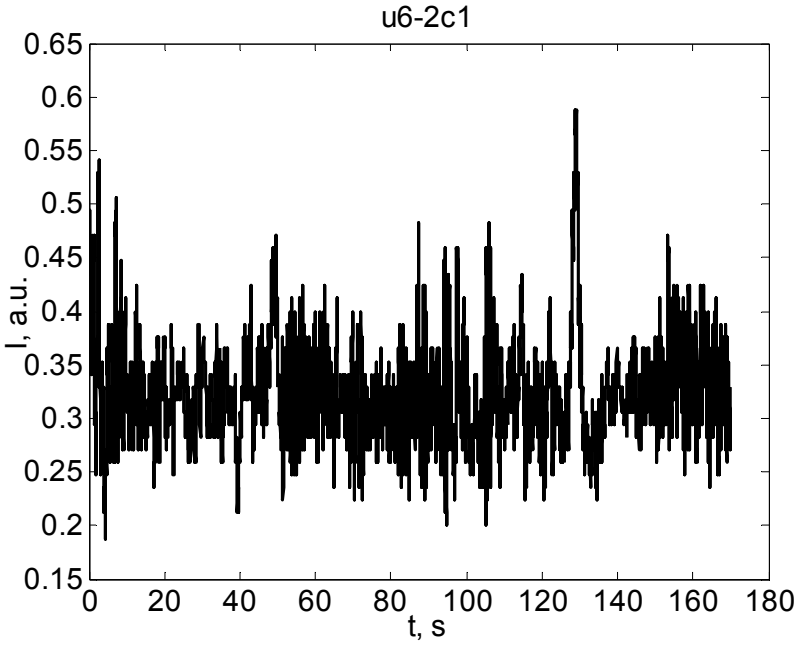

Fig. 2. A sequence of a time series recorded for sample u6-2.
(The c1 suffix is added automatically by the data processing procedure).

The Lorentzian line $S(f)$ has two free parameters a_0 and a_1 and is fit to the power spectrum using a non-linear minimization procedure to minimize the distance between the data-set and the line. We notice that a_0 enters linearly, thus it only performs a scaling of the function in the range, which translates into a shift in the logarithmic representation. The a_1 parameter enters nonlinearly into the function. Its effect in the log-log scaled plot can approximately be described as a shift along the frequency axis. The possibility to fit the whole function is advantageous compared to the alternative method described in [5, 11, 15], where the $f_{\frac{1}{2}}$ (the frequency where half-maximal-height is reached) was measured, since it takes more data points into account, thus increasing the quality of the fit.

Once the fit is completed and the parameters are found, the diameter of the SCs can be assessed as the double of the radius R. The radius can be derived as a function of the fitted parameter a_1 and other known quantities using Eq. (2):

$$R = \frac{2\mathrm{k_B}TK^2}{6\pi\eta a_1} \quad \text{where} \quad K = \frac{4\pi n}{\lambda}\sin\left(\frac{\theta}{2}\right) \tag{2}$$

In Eq. (2) k_B is Boltzman's constant, T is the absolute temperature of the sample, η is the dynamic viscosity of the solvent, θ is the scattering angle, n is the refractive index of the scattering particles and λ is the wavelength of the laser radiation.

The work described in this article was carried on using an experimental setup as described in Fig. 1. The wavelength was 633 nm, the light source was a He-Ne laser and the power was 2 mW. The DLS experiment was carried on at 20 °C. The cuvette was made of quartz and the active area length was 12 mm. The samples consisted of human urine. The cuvette-detector distance D was 1.5 m and x was 0.02 m making the scattering angle θ equal to 0°45'50". This is not typical for DLS where a big angle is chosen, usually 90°. The reason for choosing such a small angle is to shift the rollover point in the Lorentzian line towards smaller a_1 values, hence smaller frequencies, where the noise is considerably smaller.

The PSD (scattered line) and the fitted Lorentzian line for the time series recorded on sample u6-2 are presented in Fig. 3.

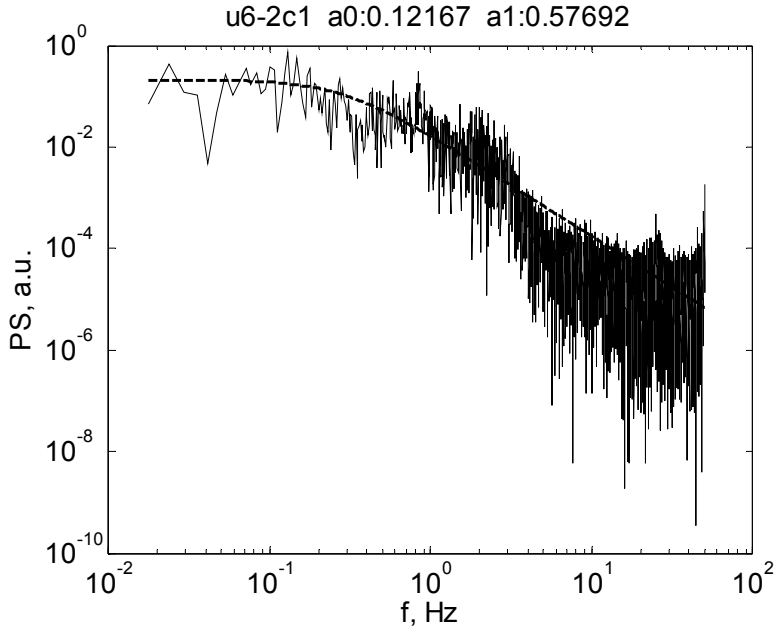

Fig. 3. The PSD (scattered line) and the fitted Lorentzian line (dashed) for the time series recorded on sample u6-2.

The parameters of the Lorentzian line found from the fit are: $a_0 = 0.122$ and $a_1 = 0.577$. Using Eq. (2) we found that the SCs have an average diameter of 50.9×10^{-9} m, which is very small. Other samples presented bigger particles in suspension. The PSD (scattered line) and the fitted Lorentzian line for the time

series recorded on sample u6-12 are presented in Fig. 4. The parameters of the Lorentzian line found from the fit are: $a_0 = 4.0$ and $a_1 = 0.109$. Using Eq. (2) we found that the SCs in sample u6-12 have an average diameter of 269×10^{-9} m, around 0.27 μm, which is much bigger than the average diameter of the SCs in sample u6-2.

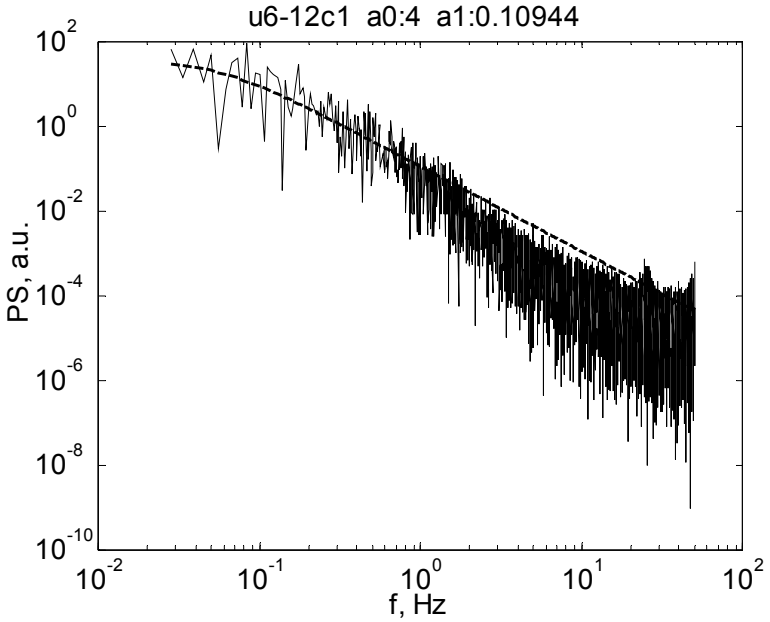

Fig. 4. The PSD (scattered line) and the fitted Lorentzian line (dashed) for the time series recorded on sample u6-12.

We should notice, however, that the diameter we measured using the procedure described above, which is basically a DLS, using non-typical values for the experimental parameters and for the detection system, is the hydrodynamic diameter, which is slightly different from the physical diameter. Moreover, the presence of particles with a wide diameter distribution changes the shape of the PSD departing it from the theoretical shape, as presented in Fig. 4.

RESULTS

Urine samples from 35 patients, both healthy and patients who asked for a medical examination, males and females, were analyzed using the procedure presented in the previous section. The sample was analyzed using the manual standard laboratory examination for urine. The lab results indicated the presence or

absence of albumin, puss, urobilinogen, glucose and sediment. The time elapsed from collecting the samples to recording the time series was less than 24 hours and does not change the results of the standard manual laboratory urine analysis or of the calcium oxalate amount in urine, as stated in [3].

The presence of albumin in urine indicates alteration of the anatomic glomerular renal filter and is always clinically significant for diagnosis and prognosis of liver involving diseases. The abnormal presence of urobilinogen (metabolism product of haemoglobin, during red blood cell turnover), is significant for hepatic cells damage [2]. Pyuria, or puss presence in urine, is always clinically significant for genito-urinary infection [2]. Renal glucosuria is glucose in the urine without hyperglycemia. It occurs with all kind of renal tubule disorders and is asymptomatic. Isolated renal glucosuria is benign [2].

Sediment in urine can consist of epithelial cells, red blood cells (RBC), white blood cells (WBC), crystals and casts. These can be identified by microscopic analysis. Epithelial cells frequently appear in urine. Only renal tubular cells are diagnostically important. The presence of cells suggests tubular injury, when in big amount or when grouped in casts. RBC presence should be interpreted in clinical context since they can originate in glomerular and nonglomerular tissue. WBC in small amount may be normal. Calcium oxalate crystals are among the four most common types of crystals in urine. They occur in large number in ethylene glycol poisoning, in high doses of vitamin C or, rarely in other disorders. These crystals are also important in evaluation of calculi [2].

Table 1

The standard laboratory urine analysis and the DLS diameter measurement

Diameter (μm)	Albumin	RBC, Bacteria	Puss, WBC	Epithelial cells	Crystals, Casts
<0.04	Absent	Absent	Absent	Absent	Absent
0.04–1	Present	Absent	Absent	Absent	Absent
1–10	Present in some samples	present	absent	Absent	Absent
11–19	Present in some samples	Present in some samples	Present	Absent	Absent
20–30	Present in some samples	Present in some samples	Present in some samples	Present	Absent
>30	Present in some samples	Present in some samples	Present in some samples	Present in some samples	Very big crystals and casts are present

The diameter measured using the procedure described in the previous section for the 35 samples was found to be in the range 0.009–40 μm, but we must note that the precision in measuring the very big diameters is small, as the data density

in the small frequency area f the PSD is small. The presence or absence of both urobilinogen and glucose in urine could not be correlated with the diameter range we measured for the 35 samples. The explanation lays in the relatively low data acquisition rate, which was 100 Hz. The urobilinogen size is much smaller than the size of proteins (albumin) [23] and the time fluctuations produced by these SC are faster, leading to a rollover frequency bigger than what could be measured precisely using a 100 Hz data acquisition rate.

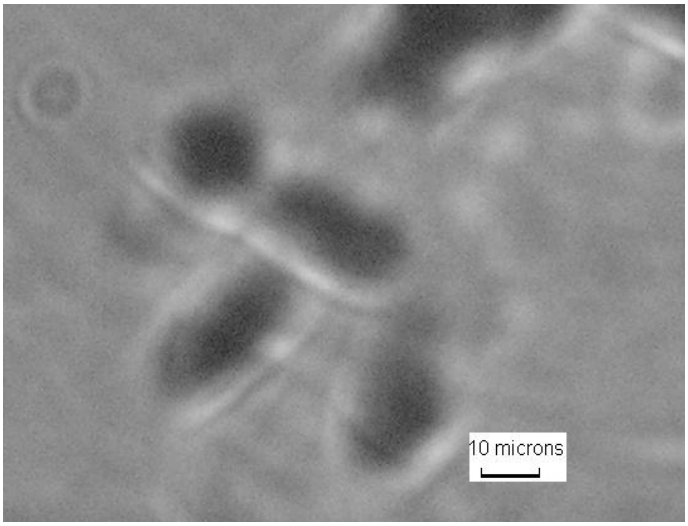

Fig. 5. Oxalate crystals in sample u26, revealed by optical microscope photograph.

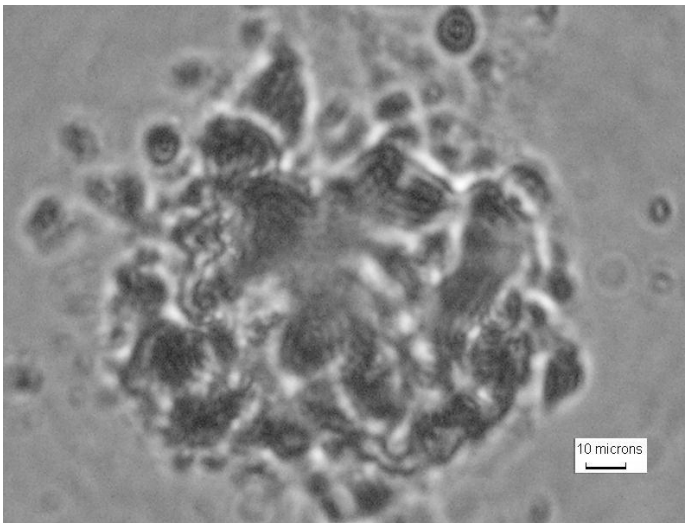

Fig. 6. Albumin conglomerate in sample u27, revealed by optical microscope photograph.

These results of the DLS diameter measurement and the results of the standard laboratory urine analysis are synthetically presented in Table 1.

The existence of micron sized SCs in samples can be probed and confirmed using an optical microscope. The presence of oxalate crystals in sample u26 is illustrated in Fig. 5. The DLS calculated diameter for sample u27 was 40 μm, caused by the big albumin conglomerates present in the sample, as revealed by Fig. 6.

These results are consistent with the biological data. Albumin is the main protein in the blood. Proteins in the blood also perform a number of important functions. They protect the body from infection, help blood clot, and keep the right amount of fluid circulating throughout the body. As blood passes through healthy kidneys, they filter out the waste products and leave in the things the body needs, like albumin and other proteins. Most proteins are too big to pass through the kidneys' filters into the urine. However, proteins from the blood can leak into the urine when the filters of the kidney, called glomeruli, are damaged [1]. The molecular dimensions of human albumin are 30 × 30 × 80 Å [2], which makes the fluctuations produced by light scattered on albumin be fast. Consequently, the rollover frequency and the a_1 parameter are bigger and the SC diameter is small. Such a PSD is presented in Fig. 3.

Other scattering center that was found in urine is the red blood cell (RBC), also called erythrocyte. The typical human erythrocyte disk has a diameter of 6–8 μm and a thickness of 2 μm, much smaller than most other human cells [1]. As the diameter is considerably bigger than the diameter of albumin, the rollover frequency and the a_1 parameter are smaller.

The following scattering center that can be present in urine, in respect of the size in increasing order, is the white blood cell (WBC). There are several different types of white blood cells. The neutrophils have an average diameter of 10–12 μm [16], eosinophils 10–12 μm [8], basophils 12–15 μm [8], lymphocytes 7–8 μm [8], monocytes 14–17 μm [8], macrophage 21 μm [8]. Consequently, the rollover frequency and the a_1 parameter of the PSD are smaller than the values of the PSD of the light scattered by RBCs.

Bigger scattering centers in urine are the epithelial cells. They are often present in the urinary sediment. Squamous epithelial cells are large and irregularly shaped, with a small nucleus and fine granular cytoplasm [16]. If only epithelial cells were present in urine, the diameter measured using DLS would be bigger than 20 μm.

Following in increasing order of the size are the casts. They are a coagulum of Tamm-Horsfall mucoprotein and the trapped contents of tubule lumen, originate from the distal convoluted tubule or collecting duct during periods of urinary concentration or stasis, or when urinary pH is very low [16]. Their cylindrical shape reflects the tubule in which they were formed. The predominant cellular elements determine the type of cast: hyaline, erythrocyte, leukocyte, epithelial, granular, waxy, fatty, or broad. The diameter calculated using DLS on such a urine sample appears to be bigger than 30 μm.

The biggest scattering centers that can be found in urine are the crystals. Calcium oxalate crystals have a refractile square "envelope" shape that can vary in size. Uric acid crystals are yellow to orange-brown and may be diamond- or barrel-shaped [16]. Triple phosphate crystals may be normal but they are often associated with alkaline urine. These crystals are colorless and have a characteristic "coffin lid" appearance. Cystine crystals are colorless, have a hexagonal shape, and are present in acidic urine, which is diagnostic of cystinuria. These very big scattering centers, as compared with the wavelength of the laser beam, produce very slow fluctuations and the output of the DLS has a bigger diameter.

As most of the particles in suspension in urine are in the range of microns, the intensity of the scattered light is proportional to the square of the diameter. A particle having the diameter equal to one micron will scatter light with intensity 100 times bigger than a particle having the diameter equal to 0.1 μm. With this in mind we understand that when big particles are present, the interference field landscape is dominated by the light scattered by the biggest particles, therefore the DLS technique yields information on the diameter of the bigger scattering centers, not on the average diameter.

Going back to Table 1, knowing the average size of the possible scattering centers, we can understand the results. Once bigger cells, as RBC or bacteria and then even bigger, like WBC or puss cells are present, albumin presence can no longer be made evident by this technique. If sediments are present, puss or WBC presence can no longer be made evident using DLS. If casts are present, the light scattered by them covers the interference landscape produced by smaller scattering centers and the technique is unable to reveal the presence of smaller objects, like epithelial cells. The same happens when conglomerates or crystals are present.

Moreover, the border lines between the categories presented in Table 1 are subject to further settlement, as measurements are in progress and strongly depend on the scattering angle and on the wavelength of the coherent incident beam [4, 9]. Consequently, this simple and very fast technique presented here can be used to qualitatively identify the biggest particles present in urine, without being sensitive to all the possible particles in suspension at the same time. This technique can be made very fast though. Using a bigger data acquisition rate a 10 seconds time series contains a sufficient amount of data and the PSD calculation and the Lorentzian fit is a matter of seconds. This technique is a much faster alternative to the standard urine examination and to the light scattering analysis technique presented in [7] where the light scattering anisotropy factor g was measured and the values were correlated with the size of the scattering centers in suspension.

CONCLUSION

The light scattering time series analysis we performed on a number of 35 urine samples revealed that a simplified and modified version of the Dynamic Light Scattering technique can be used to measure the diameter of the particles in

human urine. The presence of different particles in suspension can be associated with the diameter calculation using DLS. The technique is fast, as the whole procedure can last less than 30 seconds, but it can be used to qualitatively identify the biggest particles present in urine, without being sensitive to all the possible particles in suspension at the same time. Moreover, this technique requires no consumable reactive. This makes the technique suited as a fast screening procedure that can be used to identify the samples that have big particles in suspension and that require further analysis using the standard laboratory tests, as the dip stick. The samples presenting a diameter smaller than 0.03 μm can be considered as having very small scattering centers in suspension, thus not requiring further urine laboratory analysis.

REFERENCES

1. ANTHEA, M., J. HOPKINS, C.W. MCLAUGHLIN, S.M. JOHNSON, Q.W.D. LAHART WRIGHT, *Human Biology and Health*, Englewood Cliffs Ed., New Jersey, Prentice Hall, 1993.
2. BEERS, M.H. ed. in chief, *Merk Manual of Diagnosis and Therapy*, 18th edition, The Merk Publishing Group, New Jersey, 2006.
3. BERG, W., R. BECHLER, N. LAUBE, Analytical precision of the Urolizer (R) for the determination of the BONN-Risk-Index (BRI) for calcium oxalate urolithiasis and evaluation of the influence of 24-h urine storage at moderate temperatures on BRI, *Clinical Chemistry and Laboratory Medicine*, 2009, **47** (4), 478–482.
4. BERNE, B.J., R. PECORA, *Dynamic Light Scattering*, John Wiley. & Sons, New York, 1976.
5. BRIERS, J.D., Laser Doppler, speckle and related techniques for blood perfusion mapping and imaging, *Physiol. Meas*., 2001, **22**, R35–R66.
6. CHICEA, D., L.M. CHICEA, On light scattering anisotropy of biological fluids (urine) characterization, *Romanian Journal of Physics*, 2007, **52**(3–4), 355–360.
7. CHICEA, D., R. CHICEA, L.M. CHICEA, Using CHODIN to simulate coherent light scattering dynamics on biological suspensions, *Romanian Journal of Biophysics*, 2010, **20**, 157–170.
8. DANIELS, V.G., P.R. WHEATER, H.G. BURKITT, *Functional Histology: A Text and Colour Atlas*, Edinburgh, Churchill Livingstone, 1979.
9. DUBIN, S.B., J.H. LUNACEK, G.B. BENEDEK, Observation of the spectrum of light scattered by solutions of biological macromolecules, *PNAS*, 1967, **57**(5), 1164–1171.
10. GOODMAN, J.W., Statistical properties of laser speckle patterns, in: *Laser Speckle and Related Phenomena*, Vol.9 in series *Topics in Applied Physics*, J.C. Dainty ed., Springer-Verlag, Berlin, Heidelberg, New York, Tokyo, 1984, pp. 9–77.
11. GOODMAN, J.W. *Statistical Optics*, Wiley Classics Library Edition, New York, 2000.
12. HAMMER, M.D., D. SCHWEITZER, B. MICHEL, E. THAMM, A. KOLB, Single scattering by red blood cells, *Appl. Opt*., 1998, **37**, 7410–7418.
13. HAMMER, M.D., A.N. YAROSLAVSKY, D. SCHWEITZER, A scattering phase function for blood with physiological haematocrit, *Phys. Med. Biol*., 2001, **46**, N65–69.
14. HECHT E., *Optics*, Addison-Wesley, New York, 2001.
15. LUNACEK, N.A., J.H. CLARK, G.B. BENEDEK, A study of Brownian motion using light scattering, *American Journal of Physics*, 1970, **38**(5), 575–585.
16. RABINOVITCH, A., *Urinalysis and Collection, Transportation, and Preservation of Urine Specimens: Approved Guideline*, 2nd edition, P.A. Wayne ed., National Committee for Clinical Laboratory Standards (NCCLS), U.S.A., 2001.

17. TSCHARNUTER, W., *Encyclopedia of Analytical Chemistry*, R.A. Meyers ed., John Wiley & Sons Ltd, Chichester, 2000, pp. 5469–5485.
18. TSINOPOULOS, S.T., D. POLYZOS, Scattering of He-Ne laser light by an average-sized red blood cell, *Appl. Opt*., 1999, **38**, 5499–5510.
19. STEENBERGEN, W., R. KOLKMAN, F. DE MUL, Light-scattering properties of undiluted human blood subjected to simple shear, *J.Opt. Soc. Am. A*.**,** 1999, **16**, 2959–2967.
20. SHVALOV, A.N., J.T. SOINI, A.V. CHENYSHEV, P.A. TARASOV, E. SOINI, V.P. MALTSEV, Light scattering properties of individual erythrocytes, *Appl. Opt*., 1999, **38**, 230–235.
21. STREEKSTRA, G.J., A.G. HOEKSTRA, E.J. NIJHOF, R.M. HEETHAAR, Light-scattering by red blood cells in ektacytometry: Fraunhofer versus anomalous diffraction, *Appl. Opt*., 1993, **32**, 2266–2272.
22. WEINER, B.B., Chapter 5: Particle sizing using ensemble averaging techniques, in: *Liquid- and Surface-Borne Particle Measurement Handbook*, J.Z. Knapp, T.A. Barber and A. Liebermann eds, Marcel Dekker Inc., New York, 1996, pp. 55–172.
23. ***http://www.albumin.org/.